Correspondence

M-Ary Wavelet Transform and Formulation for Perfect Reconstruction in M-Band Filter Bank

Ming-Haw Yaou and Wen-Thong Chang

Abstract—**The binary wavelet transform is generalized and extended to the M-ary biorthonormal case. The computational equivalence between the discrete wavelet analysis and the M-band multirate signal filtering is indicated. The equivalence allows the perfect reconstruction requirement in a filter bank to be investigated from the vector space decomposition/reconstruction in wavelet analysis. From the construction of the biorthonormal wavelet bases, the necessary and sufficient condition for the filters in a perfect reconstruction filter bank is formulated. Under this formulation, an additional optimization procedure is then used to model the frequency domain requirement in filter bank design.**

I. Introduction

The design of arbitrary M-band filter banks for perfect reconstruction multirate signal filtering has been studied for a long period [1]–[3]. Most methods address this issue based on the analysis of the transfer function of filter bank in either the time domain or the frequency domain. The perfect reconstruction (PR) constraint is specified by making the input and the output of the multirate system equal. Recently, the wavelet transform has attracted considerable attention. It was found [4]-[6] that the multiresolution wavelet analysis can be implemented in the structure of a filter bank. This observation has raised great interest into research about the relationship between the two subjects. In [6]–[8], the equivalence in computational structure between the binary orthonormal wavelet transform and the two-band QMF has been indicated. In [14], the orthonormal wavelet transform has also been used for the formulation of PR in a filter bank. Recently, the orthogonality is shown not to be a necessary condition for the binary wavelet analysis [9], [10]. This implies that the orthonormal (or lossless in [8]) filter bank is not the only solution for PR multirate signal filtering. More generally, the PR filter bank should be investigated from the biorthonormal wavelet analysis.

In this correspondence, the binary wavelet analysis is generalized and extended to the case of the M-ary wavelet transform. This generalization allows us to investigate the PR constraint in multirate signal filtering from the point of view of signal space decomposition/reconstruction in wavelet analysis. The necessary and sufficient condition for PR can be explicitly formulated through the vector space analysis. With this wavelet analysis, the computational characteristics of a filter bank can be made more clear, and the relationship between the decomposed signals from all the channels can be described more precisely. In Section II, we first extend the binary orthonormal wavelet analysis to the more general M-ary biorthonormal case. This is done by using $M-1$ wavelets $\Psi^i(x)_{(i=1\sim M-1)}$ and releasing the orthonormal condition to the looser biorthonormal one. From this extension, we indicate the connection between the wavelet analysis and M-band multirate signal filtering in Section III. Then, in Section IV, based on the constraints in the construction of the general biorthonormal wavelet bases, the necessary and sufficient condition for the PR of the arbitrary M-band filter bank is derived. Based on this PR condition, additional distinct requirements of the wavelets and the filter bank such as regularity and frequency response are addressed in Section V. These characteristics lead to different considerations in the practical construction of the two subjects. Finally, in Section VI, an optimization procedure is proposed for the frequency domain consideration in the PR filter bank design. Design examples are also presented.

Manuscript received May 24, 1991; revised April 26, 1994. The associate editor coordinating the review of this paper and approving it for publication was Prof. Faye Boudreau-Bartels.

The authors are with the Institute of Communication Engineering, National Chiao-Tung University, Hsinchu, Taiwan, Republic of China.

IEEE Log Number 9406032.

II. M-Ary Biorthonormal Wavelet Analysis

The basic idea of binary orthonormal wavelet analysis is to represent a function $F(x) \in L^2(\mathcal{R})$ (finite energy real function) as a limit of successive approximations, each of which is a smoothed version of $F(x)$. The analysis is performed by using a set of bases $\{\Phi_{mn}(x)\}$ to expand a continuous function $F(x)$. These bases are generated by dilating and translating a prototype function $\Phi(x)$ called the **scaling function**. In addition, the difference between two approximations can be obtained by expanding the signal with another set of bases $\{\Psi_{mn}(x)\}$, which is generated by another prototype function $\Psi(x)$ called the wavelet. In the orthonormal case, the basis sets $\{\Phi_{mn}(x)\}$ and $\{\Psi_m(x)\}$ are mutually orthogonal and both are orthonormal bases. This leads the binary orthonormal wavelet analysis to a signal projection operation that projects signals onto a subspace $\mathbf{V}_m$ spanned by $\{\Phi_{mn}(x)\}$ and its orthogonal complement $\mathbf{W}_m$ spanned by $\{\Psi_{mn}(x)\}$. From the basic concept of signal space decomposition [11], complementary subspaces only have to be disjoint. The orthonormal requirement can be released. This observation was also pointed out in [9] and [10].

To generalize the binary orthonormal framework to the M-ary biorthonormal case, two steps are involved. First, the single wavelet $\Psi(x)$ is extended to $M-1$ wavelets $\Psi^i(x)_{,(i=1\sim M-1)}$. This leads the binary wavelet analysis to the M-ary case, which projects signals onto the subspace $\mathbf{V}_m$ and the $M-1$ complementary subspaces $\mathbf{W}^i_{m,(i=1\sim M-1)}$ spanned by the bases $\{\Psi^i_{mn}(x)\}_{,(i=1\sim M-1)}$. Second, the orthogonality between the complementary subspaces is released to the looser biorthogonal case. This can be done by introducing M dual functions $\tilde{\Phi}(x)$ and $\tilde{\Psi}^i(x)_{,(i=1\sim M-1)}$ of the functions $\Phi(x)$ and $\Psi^i(x)_{,(i=1\sim M-1)}$. These dual functions generate the dual bases $\{\tilde{\Phi}_{mn}(x)\}$ and $\{\tilde{\Psi}^i_{mn}(x)\}$ such that $\{\tilde{\Phi}_{mn}(x), \Phi_{mn}(x)\}$ and $\{\tilde{\Psi}^i_{mn}(x), \Psi^i_{mn}(x)\}$ are biorthonormal bases [12]. In addition, these bases are defined as $\Phi_{mn}(x) \triangleq M^{\frac{-m}{2}}\Phi(M^{-m}x-n)$, $\tilde{\Phi}_{mn}(x) \triangleq M^{\frac{-m}{2}}\tilde{\Phi}(M^{-m}x-n)$, $\Psi^i_{mn}(x) \triangleq M^{\frac{-m}{2}}\Psi^i(M^{-m}x-n)$, and $\tilde{\Psi}^i_{mn}(x) \triangleq M^{\frac{-m}{2}}\tilde{\Psi}^i(M^{-m}x-n)_{,(i=1\sim M-1)}$.

With this generalization, the M-ary biorthonormal wavelet analysis can be expressed as

$$P_m F = \sum_n f_m[n]\Phi_{mn,(m,n\in\mathcal{Z})}$$

$$f_m[n] = \langle F(x), \tilde{\Phi}_{mn}(x)\rangle \tag{1}$$

$$Q^i_m F = \sum_n d^i_m[n]\Psi^i_{mn,(m,n\in\mathcal{Z})}$$

$$d^i_m[n] = \langle F(x), \tilde{\Psi}^i_{mn}(x)\rangle_{,(i=1\sim M-1)} \tag{2}$$

where the operator $\langle a, b\rangle$ stands for the inner product of function a and b. The signal $P_m F$ is an approximation of $F(x)$ at resolution m. The signals $Q_m^i F_{,(i=1\sim M-1)}$ are the differences between approximations $P_{m-1}F$ and $P_m F$. Applying this wavelet analysis, a continuous signal can be decomposed into its lower resolution versions and the associated $M-1$ differences (details). Each lower resolution version can be decomposed in a similar way. The original signal can also be perfectly reconstructed by summing its lower resolution versions and details together. The perfect decomposition/reconstruction property is promised by the biorthogonality of the embedded closed subspaces defined as $\mathbf{V}_m = \text{span}\{\Phi_{mn}(x)\}$, $\tilde{\mathbf{V}}_m = \text{span}\{\tilde{\Phi}_{mn}(x)\}$, $\mathbf{W}_m^i = \text{span}\{\Psi_{mn}^i(x)\}$, and $\tilde{\mathbf{W}}_m^i = \text{span}\{\tilde{\Psi}_{mn}^i(x)\}$. The multiresolution biorthogonal space system can be expressed as

$$\begin{aligned}
&\mathbf{V}_i \subset \mathbf{V}_{j,(i>j)} \quad \tilde{\mathbf{V}}_i \subset \tilde{\mathbf{V}}_{j,(i>j)} \\
&\bigcup_{m\in\mathcal{Z}} \mathbf{V}_m = \bigcup_{m\in\mathcal{Z}} \tilde{\mathbf{V}}_m = L^2(\mathcal{R}) \\
&\bigcap_{m\in\mathcal{Z}} \mathbf{V}_m = \bigcap_{m\in\mathcal{Z}} \tilde{\mathbf{V}}_m = \{0\} \\
&\mathbf{W}_m^i \perp \tilde{\mathbf{V}}_m \quad \tilde{\mathbf{W}}_m^i \perp \mathbf{V}_m \quad \mathbf{W}_m^i \perp \tilde{\mathbf{W}}_{m,(i\neq j)}^j \\
&\mathbf{V}_{m-1} = \mathbf{V}_m \bigoplus_{i=1}^{M-1} \mathbf{W}_m^i \quad \tilde{\mathbf{V}}_{m-1} = \tilde{\mathbf{V}}_m \bigoplus_{i=1}^{M-1} \tilde{\mathbf{W}}_m^i. \qquad (3)
\end{aligned}$$

To satisfy the biorthogonal requirement, the corresponding and the bases can be described as

$$\begin{aligned}
&\langle \Phi_{mk}, \tilde{\Phi}_{ml}\rangle = \delta_{kl} \quad \langle \Psi_{mk}^i, \tilde{\Psi}_{ml}^i\rangle = \delta_{kl,(i=1\sim M-1)} \\
&\langle \Phi_{mk}, \tilde{\Psi}_{ml}^i\rangle = 0 \quad \langle \tilde{\Phi}_{mk}, \Psi_{ml}^i\rangle = 0_{,(1\sim i,j\sim M-1)} \\
&\langle \Psi_{mk}^i, \tilde{\Psi}_{ml}^j\rangle = 0_{,(i\neq j)}. \qquad (4)
\end{aligned}$$

From the embedded closed property of the projection spaces, the prototype functions $\Phi(x) \in \mathbf{V}_0$ and $\Psi^i(x) \in \mathbf{W}_0^i$ can be expanded by the wavelet basis $\Phi_{-1n}(x) \triangleq M^{\frac{1}{2}}\Phi(Mx-n)$ of subspace $\mathbf{V}_{-1}$, i.e., $\Phi(x)$ and $\Psi^i(x)$ can be represented as the linear combination of the wavelet basis $\Phi_{-1n}(x)$. That is

$$\begin{aligned}
\Phi(x) &= M^{\frac{1}{2}} \sum_n g_0(n)\Phi(Mx-n) \\
\Psi^i(x) &= M^{\frac{1}{2}} \sum_n g_i(n)\Phi(Mx-n)_{,(i=1\sim M-1)} \qquad (5) \\
g_0[n] &= M^{\frac{1}{2}}\langle \Phi(x), \tilde{\Phi}(Mx-n)\rangle \\
g_i[n] &= M^{\frac{1}{2}}\langle \Psi^i(x), \tilde{\Phi}(Mx-n)\rangle_{,(i=1\sim M-1)}. \qquad (6)
\end{aligned}$$

Similar results can be derived for the dual prototype functions $\tilde{\Phi}(x)$ and $\tilde{\Psi}^i(x)$

$$\begin{aligned}
\tilde{\Phi}(x) &= M^{\frac{1}{2}} \sum_n h_0(n)\tilde{\Phi}(Mx-n) \\
\tilde{\Psi}^i(x) &= M^{\frac{1}{2}} \sum_n h_i(n)\Phi(Mx-n)_{,(i=1\sim M-1)} \qquad (7) \\
h_0[n] &= M^{\frac{1}{2}}\langle \tilde{\Phi}(x), \Phi(Mx+n)\rangle \\
h_i[n] &= M^{\frac{1}{2}}\langle \tilde{\Psi}^i(x), \Phi(Mx+n)\rangle_{,(i=1\sim M-1)}. \qquad (8)
\end{aligned}$$

Equations (5) and (7) indicate that the prototype functions are characterized simply by the time-scale versions of the two scaling functions $\Phi(x)$ and $\tilde{\Phi}(x)$ (in orthonormal case by one scaling function $\Phi(x)$ only). This time-scale property plays an important role in the derivations of wavelet bases.

III. Filter Bank Structure in Discrete Wavelet Analysis

The discrete sequences $f_m[n]$ and $d_m^i[n]$ in (1) and (2) are the discrete approximations of the continuous signals $P_m F$ and $Q_m^i F$. The multiresolution wavelet analysis can be exactly characterized by these discrete sequences. This discrete property maps the analysis signal space from $L^2(\mathcal{R})$ onto $l^2(\mathcal{Z})$ (finite energy sequences) and provides a powerful tool to deal with sampled signals. The decomposition of a discrete sequence $f_{m-1}[n]$ into the lower resolution sequence $f_m[n]$ and $d_m^i[n]$ can be expressed as

$$\begin{aligned}
f_m[n] &= \sum_k h_0[k-Mn] f_{m-1}[k] \\
d_m^i[n] &= \sum_k h_i[k-Mn] f_{m-1}[k]_{,(i=1\sim M-1)}. \qquad (9)
\end{aligned}$$

This result can be easily derived by taking the inner product of $F(x)$ with both sides of (7). In addition, applying (5) and the fact that $f_{m-1}[n] = \langle F(x), \tilde{\Phi}_{m-1n}(x)\rangle = \langle P_m F + Q_m F, \tilde{\Phi}_{m-1n}(x)\rangle$, the reconstruction of $f_{m-1}[n]$ from $f_m[n]$ and $d_m^i[n]$ can be derived as

$$\begin{aligned}
f_{m-1}[n] &= \sum_k f_m[k] g_0[n-Mk] \\
&\quad + \sum_{i=1}^{M-1} \left\{ \sum_k d_m^i[k] g_i[n-Mk] \right\}. \qquad (10)
\end{aligned}$$

The sequences $g_i[n]$ and $h_i[n]$ are simply the coefficient sequences in the time-scale property described in (6) and (8). Equations (9) and (10) define the relationship between the discrete signal $f_{m-1}[n]$ and its lower resolution signals $f_m[n]$ and $d_m^i[n]$ in the M-ary case. These two equations establish the M-ary discrete biorthonormal wavelet analysis. This discrete analysis can be interpreted as a discrete signal decomposition/reconstruction process performed by the two sets of discrete sequences $h_i[n]$ and $g_i[n]$. In decomposition, a discrete signal $f_{m-1}[n]$ is convolved with the M sequences $h_i[-n]_{,(i=0\sim M-1)}$ to generate M subsignals. Then, the M subsignals are subsampled subsequently to obtain the lower resolution discrete signals $f_m[n]$ and $d_m^i[n]$. In reconstruction, the lower resolution discrete signals are first upsampled and convolved with the M sequences $g_i[n]_{,(i=0\sim M-1)}$. Then, the M convolved signals are combined to reconstruct the original signal. With these digital filtering notations, the decomposition and reconstruction of $f_{m-1}[n]$ by the discrete wavelet analysis can be represented by a filter bank-like structure as illustrated in Fig. 1.

By representing the discrete wavelet analysis in a filter bank-like structure, the connection between the wavelet analysis and multirate signal filtering can be easily observed. In this representation, the discrete sequences $h_i[-n]$ and $g_i[n]$ can be treated as the analysis filters and the synthesis filters in the M-band multirate filter bank. On the other hand, the filtering and sampling operations in a filter bank can also be described from the signal projection and recombination point of view. This interpretation enables the construction of PR multirate signal filtering directly in terms of the signal space analysis.

IV. Bases Construction and PR Condition

As illustrated in Fig. 1, the discrete M-ary wavelet analysis can be processed in a filter bank structure with critical sampling factor M. From the discussion in Section II, the coefficient sequences $h_i[n]$ and $g_i[n]$ in the time-scale property will uniquely determine the prototype functions and, consequently, the wavelet bases used in the continuous wavelet analysis. In addition, it has been shown that the analysis and synthesis filters are exactly the same as the sequences $h_i[n]$ and $g_i[n]$. Thus, it is clear that these filters in the multirate signal filtering can be uniquely determined from the wavelet bases in the wavelet analysis. This observation allows us to investigate the PR condition in multirate filtering from the signal space projection point of view. As discussed in Section II, the signal decomposition/reconstruction in wavelet analysis is promised by partioning the signal space

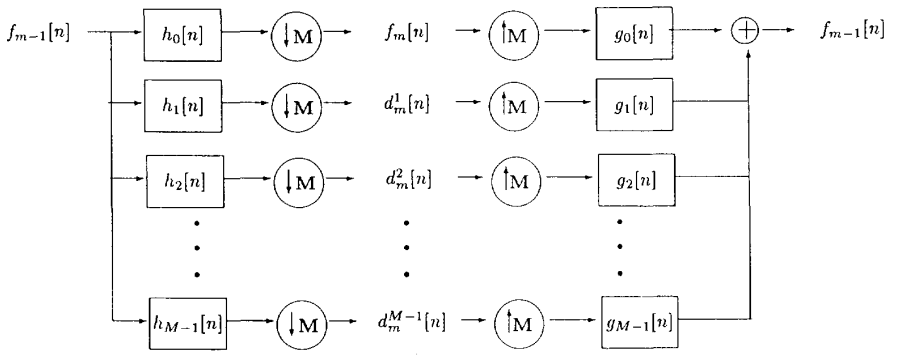

Fig. 1. Filter bank structure in M-ary biorthonormal wavelet transform.

into a family of embedded closed subspaces and the associated complementary subspaces, i.e., to construct the wavelet bases as the biorthonormal system described in (4). It can be proven by induction that the biorthonormal basis construction is equivalent to the following constraints:

$$\langle \Phi(x-k), \tilde{\Phi}(x-l)\rangle = \delta_{kl} \quad \langle \Psi^i(x-k), \tilde{\Psi}^j(x-l)\rangle = \delta_{kl}\delta_{ij}$$
$$\langle \Phi(x-k), \tilde{\Psi}^i(x-l)\rangle = 0 \quad \langle \Psi^i(x-k), \tilde{\Phi}(x-l)\rangle = 0. \tag{11}$$

Substituting the time-scale property of the prototype functions described in (5) and (7) into the above equations, the constraints on the filters $g_i[n]$ and $h_i[-n]$ can be derived as

$$\sum_n g_i[n]h_j[Mp-n] = \delta_{i,j}\delta_{p,(0\sim i,j\sim M-1,p\in Z)}. \tag{12}$$

This compact result indicates the necessary and sufficient condition for PR requirement in the general M-band multirate signal filtering. Equation (14) is derived based on the general biorthonormal wavelet analysis. As described in Section II, in its special orthonormal case, the biorthonormal wavelet basis system will become one orthonormal basis set. It leads the two sets of dual prototype functions to be identical. Therefore, the special orthonormal case of (14) can be written as

$$\sum_n g_i[n]g_j[n-Mp] = \delta_{i,j}\delta_p$$
$$h_i[n] = g_i[-n]_{,(0\sim i,j\sim M-1,p\in Z)}. \tag{13}$$

In this orthonormal case, the analysis filters $h_i[-n]_{,(i=0\sim M-1)}$ are the same as the synthesis filters $g_i[n]_{,(i=0\sim M-1)}$ with a pure time reverse. It can be seen that this result is the same as the paraunitary condition derived in [1]. However, based on the concept of wavelet analysis, both this orthonormal condition and the more general biorthonormal condition can be explicitly derived. In the general biorthonormal case, the M-ary wavelet analysis leads to the M-band PR critical sampling filter bank that decomposes signals into M disjoint subspaces. In the special orthonormal case, the biorthonormal wavelet basis system will merge into one orthonormal bases set. This leads to the PR filter bank with identical analysis and synthesis filters, which decomposes signals into M mutually orthogonal subspaces. A further discussion of the signal projection property in multirate signal filtering can be found in [15]. From the point of view of signal space projection, the PR property can be formally discussed under the concept of disjoint signal space decomposition/reconstruction. This allows us to derive the necessary and sufficient condition explicitly, although it is not obvious in other approaches.

V. Practical Considerations on Wavelets and Filter Banks

As discussed previously, the wavelet bases are uniquely determined by the scaling functions $\Phi(x)$, $\tilde{\Phi}(x)$ and the wavelets $\Psi^i(x)$, $\tilde{\Psi}^i(x)$. From the time-scale property, these prototype functions are determined by the sequences $h_i[n]$ and $g_i[n]$. Therefore, $h_i[n]$ and $g_i[n]$ will uniquely determine the wavelet bases. However, several important properties need be considered for practical applications. Taking the Fourier transform of (5) and (7), we have

$$\hat{\Phi}(w) = M^{\frac{-1}{2}} G_0\left(\frac{w}{M}\right)\hat{\Phi}\left(\frac{w}{M}\right)$$
$$\hat{\tilde{\Phi}}(w) = M^{\frac{-1}{2}} H_0\left(\frac{w}{M}\right)\hat{\tilde{\Phi}}\left(\frac{w}{M}\right)$$
$$\hat{\Psi}^i(w) = M^{\frac{-1}{2}} G_i\left(\frac{w}{M}\right)\hat{\Psi}^i\left(\frac{w}{M}\right)$$
$$\hat{\tilde{\Psi}}^i(w) = M^{\frac{-1}{2}} H_i\left(\frac{w}{M}\right)\hat{\tilde{\Psi}}^i\left(\frac{w}{M}\right). \tag{14}$$

Normalizing the scaling functions $\Phi(x)$ and $\tilde{\Phi}(x)$ by $\int_{-\infty}^{+\infty}\Phi(x)dx = \int_{-\infty}^{+\infty}\tilde{\Phi}(x)dx = 1$ and applying the above equations iteratively, one obtains

$$\hat{\Phi}(w) = \prod_{k=1}^{\infty} M^{\frac{-1}{2}} G_0(M^{-k}w)$$
$$\hat{\tilde{\Phi}}(w) = \prod_{k=1}^{\infty} M^{\frac{-1}{2}} H_0(M^{-k}w)$$
$$\hat{\Psi}^i(w) = \prod_{k=1}^{\infty} M^{\frac{-1}{2}} G_i(M^{-k}w)$$
$$\hat{\tilde{\Psi}}^i(w) = \prod_{k=1}^{\infty} M^{\frac{-1}{2}} H_i(M^{-k}w). \tag{15}$$

This result indicates that the scaling functions and wavelets can be generated iteratively from the Fourier transforms of $h_i[n]$ and $g_i[n]$, which are the filters to be derived for a PR filter bank. In fact, most of the existing wavelets are generated using this method [6], [9], [10]. In (15), the basic requirement of the iterative method is to make sure that the iteration will converge. This implies that certain constraints on regularity are needed for deriving useful wavelets. Various method have be proposed [6], [9], [10], [13] to address this regularity requirement. Basically, these methods require the frequency responses of the low-pass filters $h_0[-n]$ and $g_0[n]$ to have as many zeros as possible at the frequency π. It was also indicated that the converged functions are better at being compactly supported. This can be done by forcing the filters $h_i[n]$ and $g_i[n]$ to be FIR filters.

On the other hand, there exist some distinct requirements in the design of filter bank. Besides the PR requirement, the frequency responses of the analysis and the synthesis filters in a filter bank are

TABLE I
EXAMPLE OF A THREE-BAND BIORTHONORMAL FILTER BANK: IMPULSE RESPONSE OF THE ANALYSIS FILTERS $h_i[n]_{,(i=0\sim2)}$ AND THE SYNTHESIS FILTERS $g_i[n]$, $(i = 0\sim2)$

n	Filter $h_0[n]$	Filter $h_1[n]$	Filter $h_2[n]$	Filter $g_0[n]$	Filter $g_1[n]$	Filter $g_2[n]$
0	-7.42562725e-02	3.99934162e-02	7.42562725e-02	-5.83514617e-14	-1.58638722e-15	-5.83514617e-14
1	7.24729426e-15	-7.30333599e-17	7.24729426e-15	4.49312080e-02	1.66848663e-01	-4.49312080e-02
2	9.72845167e-02	-5.23961146e-02	-9.72845167e-02	6.01652556e-14	1.62244425e-15	6.01652556e-14
3	2.85673313e-01	-4.43421350e-17	2.85673313e-01	-9.17550352e-02	-3.40725426e-01	9.17550352e-02
4	3.60055503e-01	-1.93920986e-01	-3.60055503e-01	-1.90767366e-02	-3.21206847e-15	-1.90767366e-02
5	2.84727239e-01	1.78298508e-15	2.84727239e-01	9.76534938e-02	3.62628909e-01	-9.76534938e-02
6	9.26590109e-02	3.82602292e-01	-9.26590109e-02	2.91868117e-01	5.08948632e-15	2.91868117e-01
7	-3.94344903e-02	-3.34538227e-15	-3.94344903e-02	3.64917884e-01	-1.76752366e-01	-3.64917884e-01
8	-8.91103410e-02	-3.67949327e-01	8.91103410e-02	2.89882106e-01	-5.92821834e-15	2.89882106e-01
9	3.20071193e-14	4.57204319e-15	3.20071193e-14	1.15506494e-01	-5.59469596e-02	-1.15506494e-01
10	4.46471453e-02	1.84354441e-01	-4.46471453e-02	4.33114553e-15	1.87926995e-15	4.33114553e-15
11	-2.90961044e-14	-4.40952469e-15	-2.90961044e-14	-6.47505158e-02	3.13626910e-02	6.47505158e-02

usually excepted to be a set of consecutive equal-bandwidth frequency channels distributed in $[0, \pi]$. This can be achieved by minimizing the stop-band energy and the pass-band ripple of the associated filter. In addition, the filters in PR multirate signal filtering are not restricted to be FIR ones. Hence, the wavelet analysis and PR filter bank have some practical differences beyond their fundamental similarity. In this correspondence, we consider only the FIR filter bank design with (12). An optimization procedure for the frequency domain consideration of filter bank design will be addressed in the next section.

VI. FREQUENCY DOMAIN OPTIMIZATION FOR THE FILTER BANK

For practical application, an optimization procedure is usually used to constrain the stop-band energy of filters. This leads the filter bank design to a constrained minimization problem as

$$\text{Minimize } \Phi \triangleq \sum_{i=0}^{M-1} \left(\int_{S_i} |H_i(w)|^2 dw + \int_{S_i} |G_i(w)|^2 dw \right)$$
$$\text{Subject to (12)} \tag{16}$$

where $S_{i,(i=0\sim M-1)}$ are the ranges of stopbands for the M frequency channels. Letting filters $h_i[n]$ and $g_i[n]$ be described as $\mathbf{h}_i = [h_i[0]h_i[1]\cdots h_i[N-1]]^T$ and $\mathbf{g}_i = [g_i[0]g_i[1]\cdots g_i[N-1]]^T$, the objective function can be reformulated as

$$\Phi = \sum_{i=0}^{M-1} \frac{1}{2}(\mathbf{h}_i^T \mathbf{Q}_i \mathbf{h}_i + \mathbf{g}_i^T \mathbf{Q}_i \mathbf{g}_i) \text{ with}$$
$$\mathbf{Q}_i = 2 \int_{S_i} (\mathbf{c}\mathbf{c}^T + \mathbf{s}\mathbf{s}^T) dw \tag{17}$$

where vector $\mathbf{c} \triangleq [\cos(0)\cos(w)\cdots\cos((N-1)w)]^T$ and vector $\mathbf{s} \triangleq [\sin(0)\sin(w)\cdots\sin((N-1)w)]^T$. Denote the constraints described in (12) as $B_k(\mathbf{h}_i, \mathbf{g}_i) = 0_{,(k=0,1,\ldots)}$ and applying the Lagrange multiplier [16], the constrained minimization problem can be expressed as the minimization of the following Lagrange function L.

$$\mathbf{L}(\mathbf{h}_i, \mathbf{g}_i, \lambda_k) = \sum_{i=0}^{M-1} \frac{1}{2}(\mathbf{h}_i^T \mathbf{Q}_i \mathbf{h}_i + \mathbf{g}_i^T \mathbf{Q}_i \mathbf{g}_i) - \sum_k \lambda_k B_k(\mathbf{h}_i, \mathbf{g}_i). \tag{18}$$

The minimization of the above Lagrange function can be achieved by forcing the first-order derivatives of the Lagrange function to be zero. Define the vector operators $\nabla_{\mathbf{h}_i} = [\frac{\partial}{\partial h_i[0]} \frac{\partial}{\partial h_i[1]} \cdots \frac{\partial}{\partial h_i[N-1]}]^T$, $\nabla_{\mathbf{g}_i} = [\frac{\partial}{\partial g_i[0]} \frac{\partial}{\partial g_i[1]} \cdots \frac{\partial}{\partial g_i[N-1]}]^T$, and $\nabla_{\lambda_i} = [\frac{\partial}{\partial \lambda_0} \frac{\partial}{\partial \lambda_1} \cdots \frac{\partial}{\partial \lambda_k}]^T$,

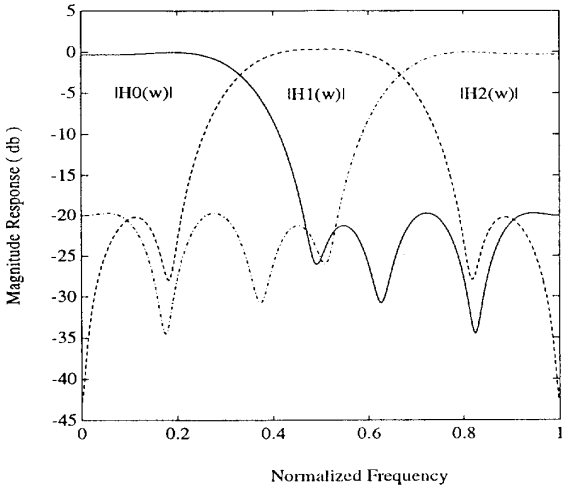

Fig. 2. Frequency response of the analysis filters listed in Table I.

and then, the first-order condition can be expressed as $\nabla_{\mathbf{h}_i}\mathbf{L} = 0$, $\nabla_{\mathbf{g}_i}\mathbf{L} = 0$, and $\nabla_{\lambda_k}\mathbf{L} = 0$. This leads the optimization problem to the following nonlinear equations:

$$\mathbf{Q}_i\mathbf{h}_i - \sum_k \lambda_k(\nabla_{\mathbf{h}_i} B_k(\mathbf{h}_i, \mathbf{g}_i)) = 0,$$
$$\mathbf{Q}_i\mathbf{g}_i - \sum_k \lambda_k(\nabla_{\mathbf{g}_i} B_k(\mathbf{h}_i, \mathbf{g}_i)) = 0, \tag{19}$$
$$B_k(\mathbf{h}_i, \mathbf{g}_i) = 0_{,(k=1,2,\ldots)}.$$

With the above derivation, the constrained minimization problem for PR filter bank design can be transferred into a system of nonlinear equations. To solve this system of nonlinear equations, Newton's method is chosen for its quick convergence. To make Newton's method more stable and to achieve a global convergence, a modified Quasi-Newton method proposed by Dennis [17] is applied for our implementation. An example of a three-band filter bank with equal-bandwidth and length 12 is shown in Table I. The frequency responses of the analysis filters and the synthesis filters are shown in Fig. 2 and Fig. 3, respectively. A test input sequence used to measure the reconstruction performance of the designed filter bank and the reconstructed output sequence are listed in Table II. The delay between the input sequence and the output sequence is equal to the order of the filters.

TABLE II
PERFORMANCE OF PERFECT RECONSTRUCTION: A TEST INPUT SEQUENCE $X[n]$ AND THE RECONSTRUCTED OUTPUT SEQUENCE $\hat{X}[n]$

n	Input Sequence $X[n]$	Output Sequence $\hat{X}[n]$	n	Input Sequence $X[n]$	Output Sequence $\hat{X}[n]$
0	1.000000	-1.90335134e-16	13	0.000000	3.00000000e-00
1	2.000000	-4.64107918e-14	14	0.000000	3.99999999e-00
2	3.000000	1.94661264e-16	15	0.000000	4.99999999e-00
3	4.000000	-2.55784976e-15	16	0.000000	6.00000000e-00
4	5.000000	-2.79869877e-13	17	0.000000	6.99999999e-00
5	6.000000	5.56325818e-15	18	0.000000	7.99999999e-00
6	7.000000	-2.31481500e-14	19	0.000000	8.99999999e-00
7	8.000000	-5.36445887e-13	20	0.000000	9.99999999e-00
8	9.000000	1.32290012e-14	21	0.000000	-2.53130849e-14
9	10.000000	-6.61970478e-14	22	0.000000	-1.34892097e-14
10	0.000000	-7.71799291e-13	23	0.000000	-5.26620473e-14
11	0.000000	1.00000000e-00	24	0.000000	-1.36213956e-13
12	0.000000	1.99999999e-00	25	0.000000	1.51545442e-14

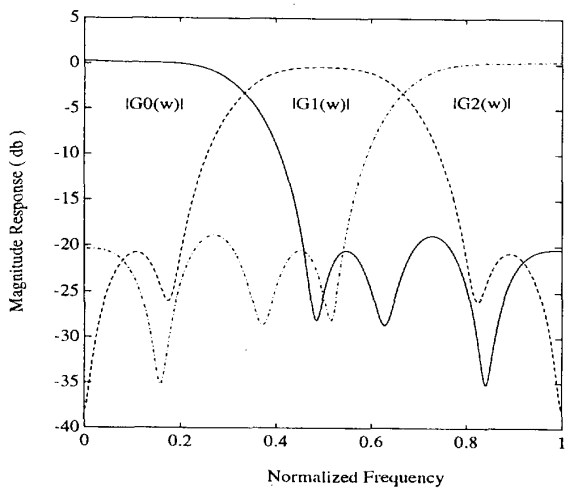

Fig. 3. Frequency response of the synthesis filters listed in Table I.

VII. CONCLUSION

By generalizing the wavelet analysis to the M-ary biorthonormal case, the equivalence in the computational structure between the arbitrary M-band multirate signal filtering and the multiresolution wavelet analysis is established. The two subjects are equivalent under the theory of multiresolution signal decomposition/reconstruction. Based on the vector space analysis, the design of the M-band filter bank can be interpreted as the construction of the wavelet bases for the multiresolution wavelet analysis with resolution step M. With this signal decomposition perspective, the operation of multirate signal filtering can be built on the concept of multiresolution signal projection. The PR problem of filter bank can then be solved directly from the constraints in the construction of wavelet bases.

REFERENCES

[1] P. P. Vaidyanathan, "Multirate digital filtering, filter bank, polyphase networks, and applications: A tutorial," *Proc. IEEE*, vol. 78, no. 1, Jan, 1990.

[2] M. Vetterli and D. L. Gall, "Perfect reconstruction FIR filter banks: Some properties and factorizations," *IEEE Trans. Acoust, Speech Signal Processing*, vol. 37, no. 7, pp. 1057–1071 July 1989.

[3] M. J. T. Smith, T. P. Barnwell, and K. Nayebi, "The time domain analysis and design of exactly reconstructing analysis/synthesis filter banks," in *Proc. IEEE ICASSP*, Apr. 1990.

[4] S. G. Mallat, "Multifrequency channel decompositions of images and wavelet models," *IEEE Trans. Signal Processing*, vol. 37, no. 12, pp. 2091–2110, Dec. 1989.

[5] ——, "A theory for multiresolution signal decomposition: The wavelet representation," *IEEE Trans. Patt. Anal. Machine Intell.*, vol. 11, no. 7, pp. 674–693, 1989.

[6] I. Daubechies, "Orthonormal bases of compactly supported wavelets," *Commun. Pure Applied Math.*, vol. XLI, pp. 909–996, 1988.

[7] G. Evangelista, "Orthogonal wavelet transform and filter bank," *Proc. IEEE 23th Asilomar Conf.* (Pacific Grove, CA), 1989, pp. 489–549.

[8] P. P. Vaidyanathan, "Lossless system in wavelet transform," *Proc. IEEE Int. Symp. Circuits Syst.* (Singapore), 1991.

[9] A. Cohen, I. Daubechies, and J-C. Feauveau, "Biorthogonal bases of compactly supported wavelets," *Commun. Pure Applied Math.*, vol. 45, pp. 485–560, 1992.

[10] C. Herley and M. Vetterli, "Wavelet and filter banks: theory and design," *IEEE Trans. Signal Processing*, vol. 40, pp. 2207–2232, 1992.

[11] R. M. Thrall, *Vector Spaces and Matrices*. New York: Wiley, 1957.

[12] J. T. Marti, *Introduction to the Theory of Bases*. New York: Springer-Verlag, 1969.

[13] H. Zou and A. Tewfik, "Design and parameterization of M-band orthonormal wavelets," *IEEE Int. Symp. Circuits Syst.*, 1992, pp. 983–986.

[14] M. H. Yaou and W. T. Chang, "Design of M-band filter banks based on wavelet transform," *Proc. SPIE, Visual Commun. Image Processing*, 1991, pp. 149–159.

[15] M. H. Yaou and W. T. Chang, "A vector space projection approach for perfect reconstruction FIR filter banks design," to appear in *J. Visual Commun. Image Representation*, vol. 5, no. 2, pp. 156–171, 1994.

[16] R. Fletcher, *Practical Methods of Optimization*. New York: Wiley, 1981.

[17] J. E. Dennis, *Numerical Methods for Unconstrained Optimization and Nonlinear Equations*. Englewood Cliffs: Prentice-Hall, 1983.